THE PROTEIN SOCIETY

The critical role of the loops of triosephosphate isomerase for its oligomerization, dynamics, and functionality

Ataur R. Katebi and Robert L. Jernigan*

Department of Biochemistry, Biophysics and Molecular Biology, LH Baker Center for Bioinformatics and Biological Statistics, Interdepartmental Program for Bioinformatics and Computational Biology, Iowa State University, Ames, Iowa 50011-3020

Received 26 August 2013; Revised 1 December 2013; Accepted 3 December 2013
DOI: 10.1002/pro.2407
Published online 8 December 2013 proteinscience.org

Abstract: Triosephosphate isomerase (TIM) catalyzes the reaction to convert dihydroxyacetone phosphate into glyceraldehyde 3-phosphate, and *vice versa*. In most organisms, its functional oligomeric state is a homodimer; however, tetramer formation in hyperthermophiles is required for functional activity. The tetrameric TIM structure also provides added stability to the structure, enabling it to function at more extreme temperatures. We apply Principal Component Analysis to find that the TIM structure space is clearly divided into two groups—the open and the closed TIM structures. The distribution of the structures in the open set is much sparser than that in the closed set, showing a greater conformational diversity of the open structures. We also apply the Elastic Network Model to four different TIM structures—an engineered monomeric structure, a dimeric structure from a mesophile—*Trypanosoma brucei*, and two tetrameric structures from hyperthermophiles *Thermotoga maritima* and *Pyrococcus woesei*. We find that dimerization not only stabilizes the structures, it also enhances their functional dynamics. Moreover, tetramerization of the hyperthermophilic structures increases their functional loop dynamics, enabling them to function in the destabilizing environment of extreme temperatures. Computations also show that the functional loop motions, especially loops 6 and 7, are highly coordinated. In summary, our computations reveal the underlying mechanism of the allosteric regulation of the functional loops of the TIM structures, and show that tetramerization of the structure as found in the hyperthermophilic organisms is required to maintain the coordination of the functional loops at a level similar to that in the dimeric mesophilic structure.

Keywords: triosephosphate isomerase; dihydroxyacetone phosphate; glyceraldehyde 3-phosphate; proton shuttling

Introduction

Triosephosphate isomerase (TIM) is the fifth enzyme in the eukaryotic glycolysis pathway, which consists of 10 sequential steps that convert one molecule of glucose into two molecules of pyruvate. In the process, it uses two ATP molecules and produces four ATP molecules with a net gain of two ATP molecules. TIM isomerizes dihydroxyacetone phosphate (DHAP) into glyceraldehyde 3-phosphate (GAP). TIM is an essential enzyme in most organisms. In all organisms, TIM is found to be in a dimeric state

Abbreviations: DHAP, dihydroxyacetone phosphate; GAP, glyceraldehyde 3-phosphate; PC, principal component; TIM, triosephosphate isomerase.

Additional Supporting Information may be found in the online version of this article.

Grant sponsor: NSF MCB; Grant number: 1021785. Grant sponsor: NIH; Grant number: R01GM072014.

*Correspondence to: Robert L. Jernigan, 112 Office & Lab Building, Iowa State University, Ames, IA 50011. E-mail: jernigan@iastate.edu

in the active enzyme except in hyperthermophilic organisms such as *Thermotoga maritime*,[1] *Pyrococcus woesei*,[2] *Thermoproteus tenax*,[3] and *Methanocaldococcus jannaschii*,[4] where its functional state is a tetramer. It has been postulated that the tetrameric form imparts additional critical stability for thermophilic organisms.[2,3] Here we will investigate the internal dynamics of the various oligomeric states to learn about their similarities and differences.

Each subunit of the TIM structure has an alpha/beta barrel architecture. The loops connecting the strands and helices play important roles in oligomerization and functionality of the enzyme. It has been found previously that loop motions (labeled as Loop 6) are not random and can be critical for the functionality of this enzyme.[5–8] It was found that this loop does not move independently but rather together with the domain motions in a highly cooperative allosteric way. Loop 6 is a flexible 11 residue component of the structure with hinge residues at both ends. The tip of this loop has a "phosphate gripper" motif,[9] which is likely engaged in substrate binding, protecting the substrate during catalysis, and product release.[10,11] We have selected 121 TIM structures from the PDB[31] for this study. The pairwise sequence identity of the structures ranges between 44.0% and 97.1%. However, the three residues (Lys on Loop 1, His on Loop 4, and Glu on Loop 6) that are responsible for catalysis are strictly conserved. This large number of diverse PDB structures provides a rich dataset to use to understand the dynamics of these structures. In this research, we find that oligomeric state of the TIM structures does affect its structural stability, functional dynamics, and functional loop coordination.

Diversity of TIM structure space

Dimeric and tetrameric TIM structures from 121 PDB Ids have been extracted, and from these we have selected 267 TIM subunits after removing chains having missing residues. Out of these 267 subunits, 198 are in open conformation and 69 are in closed conformation. The open structures have the functional Loop 6 wide open and the closed structures have this loop in a closed state covering the catalytic cavity. Moreover, the functional loops 7 and 8 in the open structures are wider open than they are in the closed conformation, but the magnitude of the conformational transition of these two loops between the open and closed states is much smaller compared to the similar transition for Loop 6. In most cases, unliganded structures are in open conformation. The exceptions can occur because of some mutations or engineering of a section of the structure. A mutation of the two hinge residues (168 and 178—residue indexing on the yeast TIM structure) on the functional Loop 6 can reduce the flexibility of the loop preventing the structure from achieving a fully open or closed conformation. Two such examples are mutation P168A (PDBs 2J24 not fully open and 2J27 not fully closed) and mutation A178L (PDBs 2V0T unliganded not fully open and 2V2C liganded not fully closed). On the other hand, most liganded structures are in closed conformation. However, some liganded TIM structures are found in an open conformation—one such example is PDB 1TSI, whose subunit A has an N-hydroxy-4-phosphono-butanamid ($C_4H_8NO_5P$) ligand but the structure is in a wide open conformation. Moreover, some engineered TIM structures fail to achieve complete functional Loop 6 flexibility and do not fully open or close (PDB 1MSS).

We have performed principal component analysis (PCA) on the superimposed subunit structures. Figure 1(A) shows the PCA of 267 subunits of the TIM PDB structures. The first and the second PCs (PC1 and PC2) divide the structures into open and closed sets. The largest variation in the data is along PC1 (84.58%). This variation arises primarily according to the extent of closedness/openness of the subunits, that is, the conformational variability of Loop 6. The 198 subunits of the open set represent a more diverse set of structures than do the 69 subunits of the closed set, which can be seen in the broader scatter of the structures in the open set. The RMSD difference between the representative open and closed structural subunits (1YPI A and 2YPI A) is 1.15Å. The range of the RMSD distribution for these two sets also shows that the span of the closed subunits is much tighter than the span of the open subunits—0 to 0.69Å (closed set) and 0–2.31Å (open set).

The not fully closed structure 2J27 is clearly positioned away from the closed cluster and more towards the open structures as shown in Figure 1(A). The rotation of catalytic residue Glu 167 is synchronized with the opening/closing of the functional Loop 6. Because of the mutation P168A adjacent to Glu 167, this structure fails to close the functional Loop 6 sufficiently so that Glu 167 is not placed into its proper catalytic position in the closed conformation.[12] On the other hand, the open structure 2J24 with the same mutation is positioned away from the open cluster as it fails to open the functional Loop 6 fully. These TIM structures are deviants from the clusters of both the open and closed TIM structures and have the functional Loop 6 in an intermediate position. This induced closedness may occur for different reasons. In the *G. gallus* TIM structure (8TIM), its partial closure is caused by a trapped sulfate ion (SO_4^{-2}) in the catalytic pocket. In the *Trypanosoma brucei* mutant (A178L) TIM structure 2V0T, its partial closure is caused by the mutation of the Loop 6 hinge residue Ala 178 to Leu.[13] In the *Plasmodium falciparum* mutant (W168F) TIM structure 1VGA, the mutation

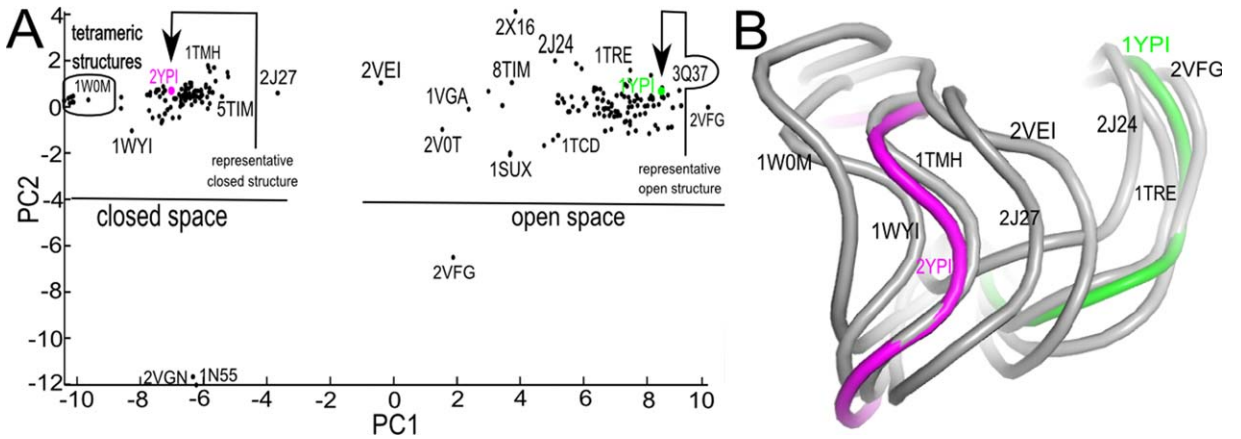

Figure 1. Distribution of the TIM experimental structures in PC space. (A) Different TIM crystal structures shown along the first two PCs, showing clearly that the closed and the open structures form distinct sets, with members of the closed set being more similar to one another than are the open structures. The distribution also indicates that the primary coordinate for this transition is along PC1. 69 structures are in closed set and 198 structures are in open set. The PDB Id for the representative closed structure is 2YPI chain A and PDB Id for the representative open structure is 1YPI chain A. PC1, PC2, and PC3, captures 84.58%, 5.46%, and 3.02%, of the total variability. Some of the data points are labeled to facilitate visualization. (B) Overlay of the functional Loop 6 region of some selected representative TIM structures distributed along PC1 from panel A. It shows the conformational transition of Loop 6 between open and closed states.

of the conserved Trp 168 into Phe causes the functional Loop 6 to adapt an intermediate conformation.[14] 2VXN and 1N55 are two closed structures that are placed further away along PC2 from the cluster of the closed structures at the bottom of the figure. No differences between 2YPI A (reference closed structure) and these two structures are visually discernible.[15] Moreover, the subunit structures from the four tetrameric closed structures form a subcluster within the cluster of the closed structures, but at the extreme left end of the PC1 axis suggesting that they are more closed than any others. Figure 1(B) shows the positions of the functional Loop 6 in the TIM structures in different conformational states along PC1. It is clear from the states of Loop 6 in panel B that 2VFG at the rightmost position in panel A has the most open form and 1W0M at the leftmost position in panel A is the most closed. The other selected structures show different intermediate states of Loop 6.

Monomeric, dimeric, and tetrameric TIM architectures

The structure of a TIM subunit follows the (α/β)-barrel architecture, with the two types of secondary structures alternating along the sequence. It has a central barrel consisting of eight β-strands (β1–β2) surrounded by eight helices α1–α8. Figure 2(A) shows this arrangement in the TIM subunit. The C-termini of the strands make the front of the barrel and the other ends of the strands constitute the back of the barrel.

There are eight loops at the front, front loops FL1–FL8; and eight loops at the back, back loops BL1–BL8. Each front loop runs from a strand to a helix, and each back loop runs from a helix to a strand. Thus the whole structure has such an arrangement of the strands, loops, and helices: N terminus-(β1-FL1-α1)-BL1-(β2-FL2-α2)-BL2-(β3-FL3-α3)-BL3-(β4-FL4-α4)-BL4-(β5-FL5-α5)-BL5-(β6-FL6-α6)-BL6-(β7-FL7-α7)-BL7-(β8-FL8-α8)-C terminus. The number of amino acids that constitute these secondary structure segments varies somewhat from one TIM structure to another. But the overall architecture of the structure is strictly conserved. Supporting Information Table SI shows the positions of the secondary structure segments in the sequences for three different organisms that have been considered—*T. brucei* TIM, *Thermotoga maritima* TIM, and *P. woesei* TIM. The front loops are grouped into two sets: the loops forming the interface (front loops 1, 2, 3, and 4) and the loops that drive the catalysis (front loops 6, 7, and 8). The loops shown in Figure 2(A) are all front loops, and this designation is dropped hereafter.[16]

In mesophilic organisms, the functional TIM enzyme is a homodimer. However TIM is found to be an active homo-tetrameric structure in some extremophilic organisms. Dimerization of TIM occurs through the association of two TIM monomers at a Type 1 interface. Two Type 1 dimeric TIM structures bind together by interactions along the two Type 2 interfaces to form a homo-tetrameric structure. The locations of these interfaces are marked in panels B, C, and D of Figure 2.

The Type 1 and Type 2 interfaces are shown in greater detail in Figure 3. Four interface loops (1, 2, 3, and 4) from each subunit take part in forming the Type 1 interface for the subunit–subunit association that is present in the dimer. Loop 3 from one

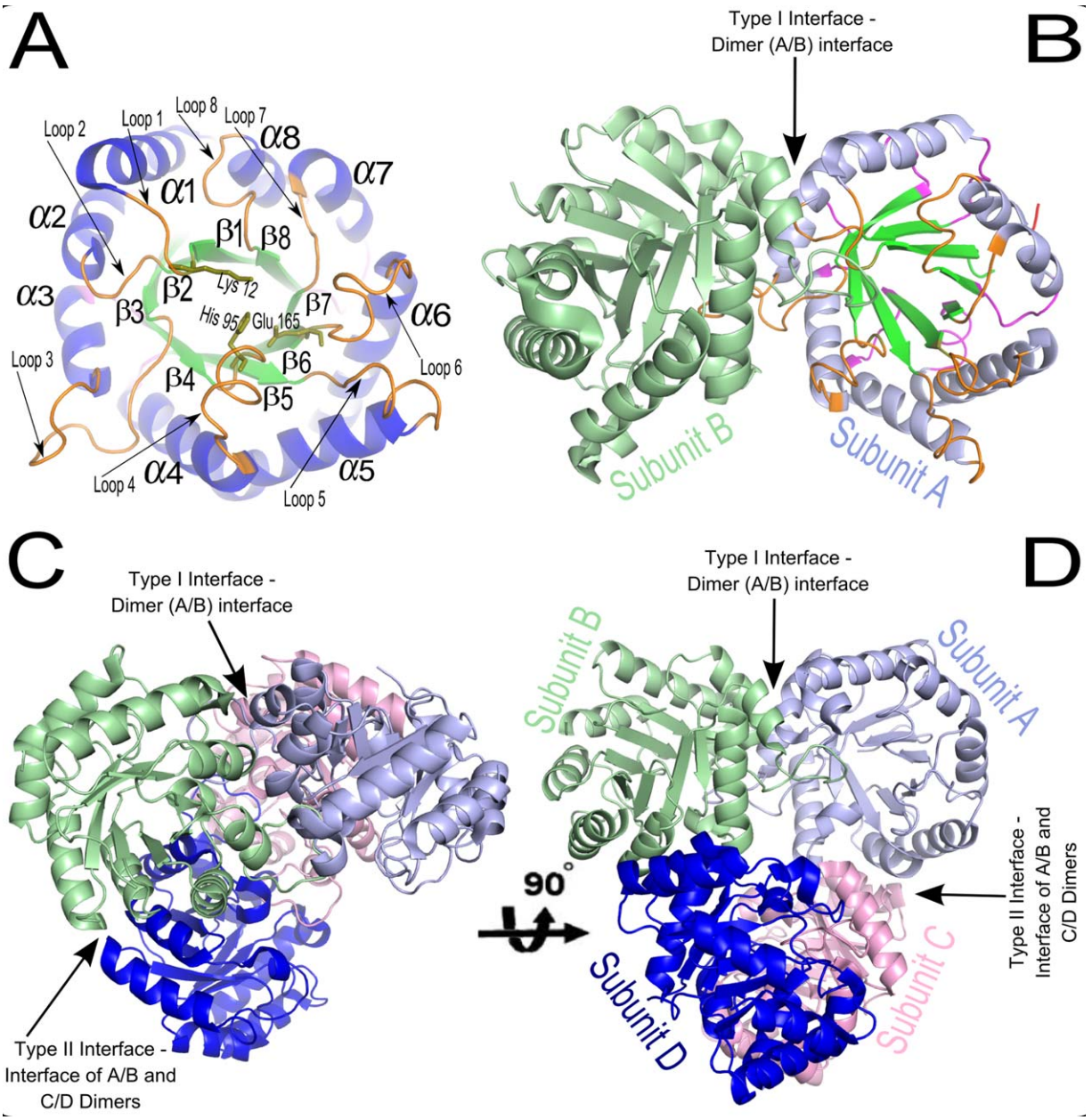

Figure 2. Structural details of TIM in the monomer, dimer, and tetramer. (A) Different structural components of a monomeric TIM subunit (based on *S. cerevisiae* TIM with PDB 1YPI). Eight strands β1–β8 form the central barrel. The helices α1–α8 surround the barrel. Front loops are labeled as Loop 1–Loop 8. The catalytic residues are labeled Lys 12, His 95, and Glu 165. (B) Dimeric TIM architecture (based on *S. cerevisiae* TIM with PDB 7TIM). A dimer is formed by the interactions along the Type 1 interface of the two subunits. (C) Tetrameric TIM structure (based on *P. woesei* TIM with PDB 1HG3).[2] Two Type 1 dimers form a tetrameric structure by the interaction along the two Type 2 interface regions. (D) The tetrameric TIM structure in panel C after a 90° rotation around the axis.

subunit docks between Loop 1 and Loop 4 of the other subunit, and Loop 2 gets buried between them. Figure 3(A,B) show details of this association. In the tetrameric organization, there are two Type 1 dimeric TIM structures bound together by two Type 2 interfaces. A Type 2 interface is formed by the association of the C-terminus of Loop 4, the N-terminus of helix 4, and helix 5 of one subunit with the same set of structural components of the interacting subunit. Figure 3(A,C) show the details of this construction.

Conserved functional mechanism across species

The function and enzyme mechanism of TIM structures are conserved across species. The four important components of this mechanism are:

i. Substrate trapping in the hydrophobic cage and product release by the concerted motions of functional loops 6 and 7.
ii. Substrate specificity facilitated by Loop 8.

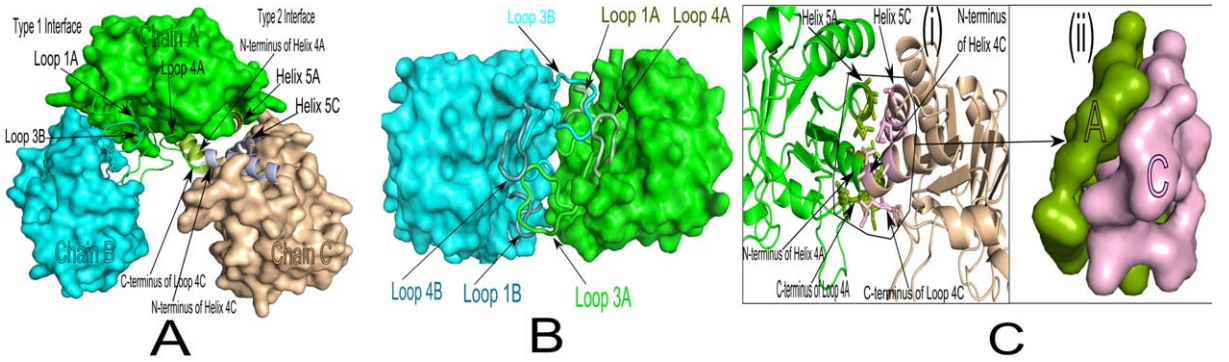

Figure 3. TIM subunit interface structures. (A) Arrangement of Type 1 and Type 2 interfaces in a tetrameric TIM structure. (B) Interdigitation of loops in Type 1 interface formation—Loop 3 of one subunit docks between Loop 1 and Loop 4 of the partner subunit. (C) (i) Structural components of the Type 2 interface—Helices 5A and 5B, N-termini of helices 4A and 4C, C-termini of Loop 4A and Loop 4C construct the Type 2 interface. (ii) Surface view of the Type 2 interface shown in (i).

iii. Catalysis of substrate—proton transfer from DHAP to GAP and vice versa.
iv. Importance of open and closed conformations to admit substrate and expel product.

Substrate trapping in the hydrophobic cage and product release by the concerted motions of functional Loop 6 and Loop 7. The rate constant of the opening and closing motion of the active site Loop 6 nearly matches the production rate for TIM catalysis. This loop motion is coordinated with substrate binding, catalytic onset, and product release.[10,11] Crystallographic studies have shown that Loop 6 and Loop 7 have a closed conformation in the presence of ligand in the catalytic cavity and an open conformation in the absence of ligand.[17,18] Figures 4(B) and 8 show the catalytic pocket of the superimposed structures of the open and closed conformations. However, experiments also show that for the substrate to be trapped (bound) in the catalytic pocket, Loop 6 closing is not necessary although the closed conformation is required for catalysis (PDBs 1LYX, 1LZO).[19]

Experiments show that perturbation of the dimerization of TIM structures reduces the rate of reaction of this enzyme by a factor of 1000 fold. Dimerization of TIM enhances the motions along Loop 6 and Loop 7 regions. It also increases the rigidity of Loop 1, Loop 4, and Loop 8. This rigidity is required to stabilize the position of the catalytic residues Lys on Loop 1 and His on Loop 4, as well as Leu on Loop 8 for the catalytic mechanism to function.[20] The active site loop dynamics is not only important for ligand release, it also limits the turnover rate of the protein.[21] Also the closing of Loop 6 (an excursion of 7Å) stabilizes the reaction enediolate intermediate. This stabilization is facilitated by

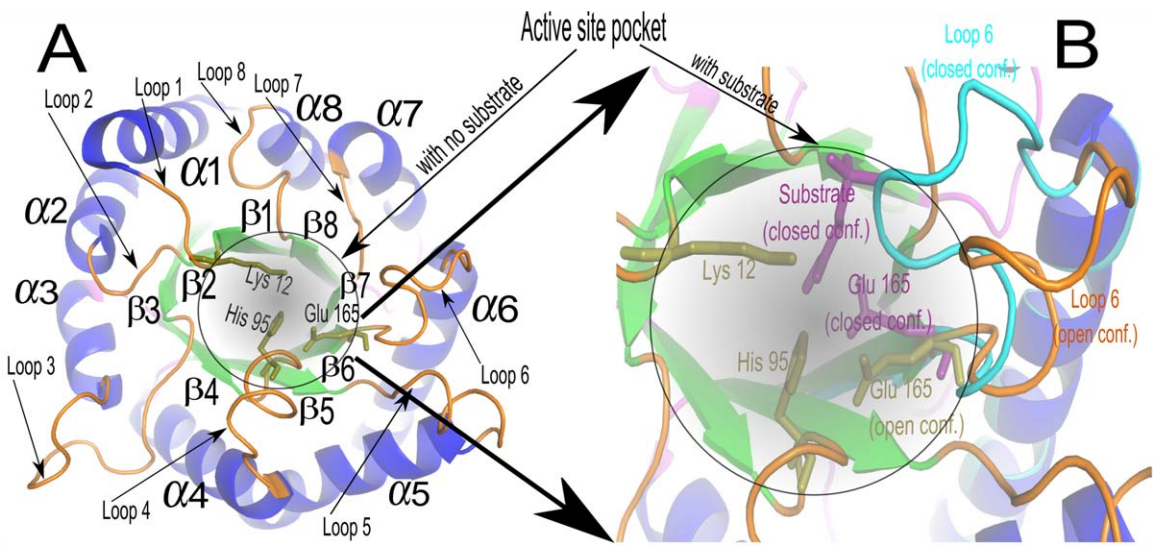

Figure 4. Structural details of the active site of TIM. (A) Location of the active site with its three catalytic residues in a TIM subunit. (B) Active site pocket is shown in enlarged view with Loop 6 in both open (orange) and closed (cyan) conformations. The structure and residue indexing are based on the *S. cerevisiae* TIM structure PDB 1YPI.

the tip of this loop which has a conserved "phosphate gripper" motif -AXGXGKXA-.[9] This motif is similar to the consensus turn that interacts with phosphate groups in some kinases, many dehydrogenases, ras p21, and other nucleotide binding proteins.[22–27]

Substrate specificity facilitated by Loop 8. While the dynamics of Loop 6 and Loop 7 appear to directly determine the catalytic activity and rate, highly conserved Loop 8 residues help to form a tight binding pocket for the phosphate moiety of the substrate. The fully conserved, solvent exposed Leu 238 (TbTIM residue indexing) of Loop 8 limits the substrate binding specificity of TIM to only DHAP and GAP (related PDB 1DKW).[28]

The following residues from loops 6, 7, and 8 form polar interactions with the phosphate oxygen of the substrate in the closed conformation of the TIM structure: Gly 173 on Loop 6; Gly 212 and Ser 213 on Loop 7; and Gly 234 and Gly 235 on Loop 8.[28]

Catalysis of the substrate—proton transfer from DHAP to GAP. Substrate catalysis in the catalytic pocket has two components. The physico-chemical structure of the catalytic cavity with proper positioning of catalytic residues is required for the proton transfer.[29] The concerted motions of Loop 6, Loop 7, and Loop 8 are likewise required.[30]

The catalytic residues Lys on Loop 1, His on Loop 4, and Glu on Loop 6 are involved in the proton transfer through their coordination. These residues in the catalytic pocket are shown in Figure 4(A,B).

The concerted motions of loops 6 and 7 are important mainly for two reasons. First, the conformational flexibility of the catalytic residue Glu on Loop 6 and its concerted motion with Loop 7 facilitate proton shuttling.[31] Second, the concerted motion of Loop 7 and the "phosphate gripper" on Loop 6 synchronize the substrate trapping with the catalytic activity.[9]

Importance of open and closed conformations to admit substrate and expel product. TIM has two distinct conformations—open and closed. In the open conformation Loop 6 is wide open and appears in a more flexible state than it is in the closed conformation, as shown in Figures 4(B) and 8. This flexibility of Loop 6 is conducive to hunting and using the phosphate gripper to bring the substrate into the vicinity of the active site. Once the substrate is trapped in the cavity, Loop 6 assumes the closed conformation, and its "phosphate gripper" maintains the substrate in place with the coordination of Leu 238 (TbTIM residue indexing) from Loop 8. The closing of Loop 6 affects the mechanism in two ways; first, it places the catalytic residue Glu 167 against the substrate at the proper distance; second, the correlated motions of loops 6 and 7 facilitate the proton transfer mechanism in a coupled manner.[10,11]

Relation between protein motions and their functions

The overall architecture of a protein is responsible for its motions particularly for the large scale domain movements but also affecting the more localized fluctuations. The way two or more domains attain their comparative movements is largely determined by the structure at the interfaces between the domains.[32,33] Domain motions are typically important for the activities of a protein: its catalysis, the regulation of its activity, transport of metabolites, and forming protein assemblages.

In this research, we apply Elastic Network Models (ENMs) to investigate the dynamics of four structures in different oligomeric assemblies: monoTIM, TbTIM monomer and dimer; TmTIM monomer, dimer, and tetramer; and PwTIM monomer, dimer, and tetramer. These have been broadly used to extract the important functional motions of proteins.[5,34–46] We measure the average fluctuations of motions for different parts of the structure focusing particularly on (1) the parts important for interface formation (front loops 1, 2, 3, and 4) and (2) the region that is important for catalysis (front loops 6, 7, and 8). We then compare these results for different monomeric states and measure and compare the correlations and overlaps of the motions of the different functional loops. From these computational results, we learn how oligomerization stabilizes the structures and also helps the structure to attain its native functional dynamics.

Results

Oligomerization and stability across the interface region

Front loops 1, 2, 3, and 4. The Type 1 interface is formed by the interdigitation of front Loop 3 with front loops 1 and 4 of the partner subunit as shown in Figure 5(A). Panel B of the figure shows how this forms a locked situation between two subunits. Front Loop 2 is buried by front Loop 3 from the partner subunit. Two such symmetric arrangements make a strong interface between the subunits to form a dimer. This dimerization locks these loops in place and reduces the dynamics of these loops. ENM captures the change of motions in functional loops 1 and 4 upon oligomerization. Figure 5(C–E) show that dimerization decreases the fluctuations of front Loop 1. Tetramerization of the structure does not impact the dynamics of the structure as much. This stabilization of Loop 1 in each oligomeric state helps stabilize the catalytic residue Lys (K13 in TbTIM,

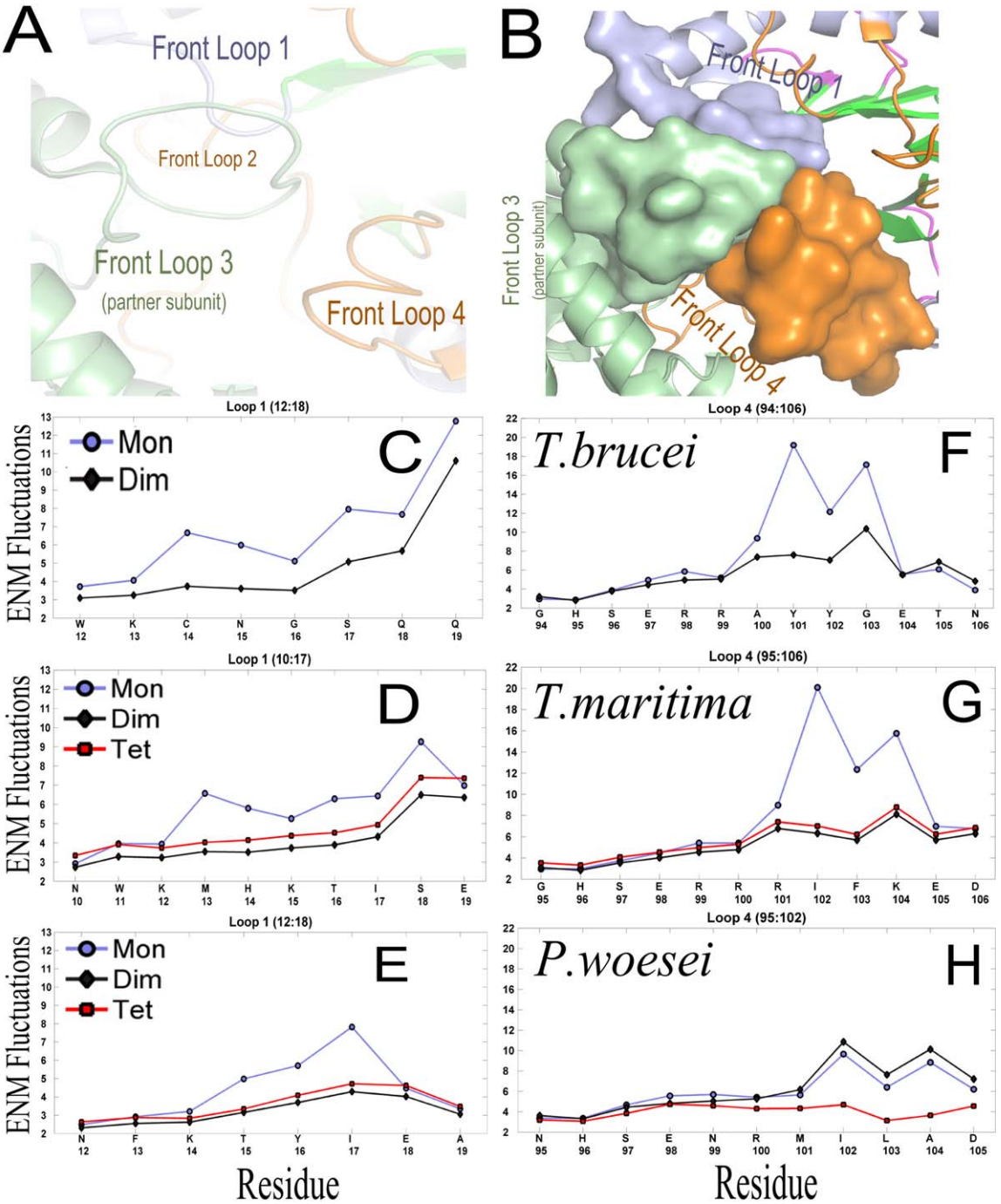

Figure 5. Dimeric interface loop fluctuations. (A) Cartoon view of interdigitation of front loops 1 and 4 with the front Loop 3 from the partner subunit. (B) Surface view shows the docking of front Loop 3 between the ridges of front loops 1 and 4 of the partner subunit. (C, D, E, F, G, and H) Fluctuations of the two front loops 1 and 4 are shown in different oligomeric states in three different organisms and in an engineered monomer.

K12 in TmTIM, and K14 in PwTIM) on this loop. Figure 5(F) shows that the C-terminus of Loop 4 is stabilized upon dimerization in *T. brucei* TIM. While tetramerization in *T. maritima* TIM does not affect the fluctuation of this loop as much [Figure 5(G)], tetramerization in *P. woesei* TIM reduces the fluctuation of the C-terminus of this loop [Figure 5(H)]. This decrement of motion stabilizes the catalytic residues Lys on Loop 1 and His on Loop 4, as required for catalysis.[10,11]

Panels A, B, and C of Figure 6 show the reduced fluctuations of Loop 2 after dimerization. Panels D, E, and F of Figure 6 show the reduced fluctuations of Loop 3 from the partner subunit after dimerization. Front Loop 3 is the longest loop in the TIM structures and has the highest mobility in the

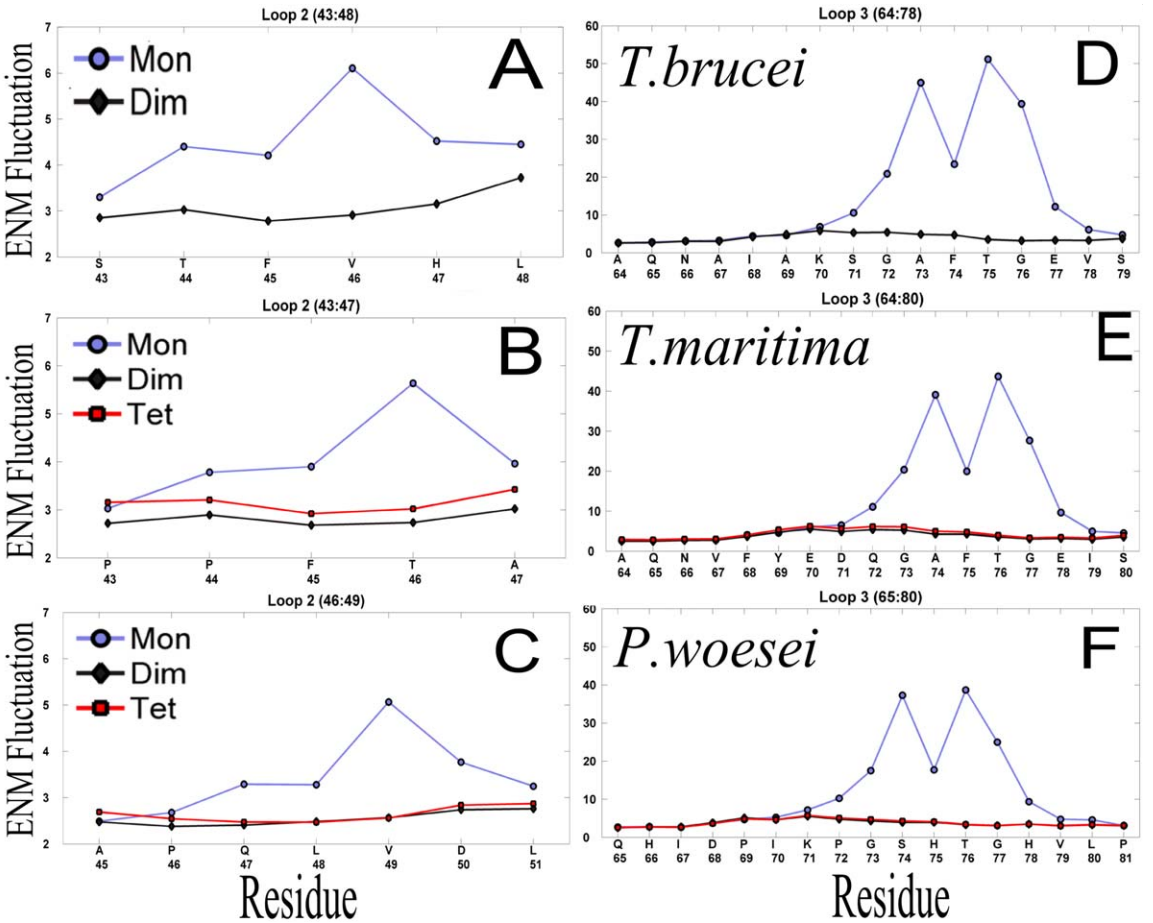

Figure 6. Changes in fluctuations of interface loops 2 and 3 in different oligomeric states. Supporting Information Figure 1 compares the fluctuations of front Loop 8 in different oligomeric states for *T. brucei*, *T. maritima*, and *P. woesei*. It is clear that fluctuation of this loop increases upon tetramerization in the hyperthermophilic structures. Experiments show that the highly conserved Loop 8 helps the TIM structure maintain a tight binding catalytic pocket. Especially, L238 in *T. brucei* TIM and L239 in *T. maritima* TIM help maintain the high substrate specificity.[20] However, in case of *P. woesei* TIM this is replaced by K210. Higher fluctuations of Loop 8 may cause Leu to come out of its buried position to make room for the substrate to become properly positioned within the pocket.

isolated subunit. Dimerization causes a large reduction in the mobility of this loop.

Dimerization lowers the fluctuations of the interface loops 1, 2, 3, and 4 of each subunit in the TIM structures and this reduction of mobility in the interface loops heightens the catalytically important fluctuations along the functional loops 6, 7, and 8. The next section will delve into the details of the motions of these functional loops upon oligomerization.

Oligomerization and functional loop motions along the catalytic pocket

Front loops 6, 7, and 8. Front loops 6, 7, and 8 surround the catalytic pocket. Figure 7(A) shows the functional loops in the open conformation of the structure (*Saccharomyces cerevisiae* PDB 1YPI). Here the substrate is copied over from the closed TIM structure of the same organism (PDB 7TIM) whose catalytic site is shown in Figure 7(B). Functional Loop 6 closes over the catalytic pocket in the closed conformation. The "phosphate gripper" forms the tip of this loop. This consists of the following residues: 169-AIGTGLAA-176 in *T. brucei* TIM. By switching from open to the closed conformation, this "gripper" region makes a large excursion towards the catalytic cavity—G173 making the largest movement of 8.0Å; and this motion for the residues on both sides of it in the loop is reduced as you move away along the sequence, as shown in Figure 8. This conformational change of the "phosphate gripper" is important.[9] In the open conformation, this region is disordered and may actively recruit substrate. Once the substrate is placed in the pocket, this loop stays in a closed conformation by covering the opening of the catalytic pocket and thus protecting the catalytic mechanism from water invasion or other molecules.[17,18]

Panels C, D, and E of Figure 7 show the change in the fluctuations of front Loop 6 upon oligomerization in *T. brucei*, *T. maritima*, and *P. woesei*, respectively. There are two important points in these figures. First, Loop 6 in panel C has higher

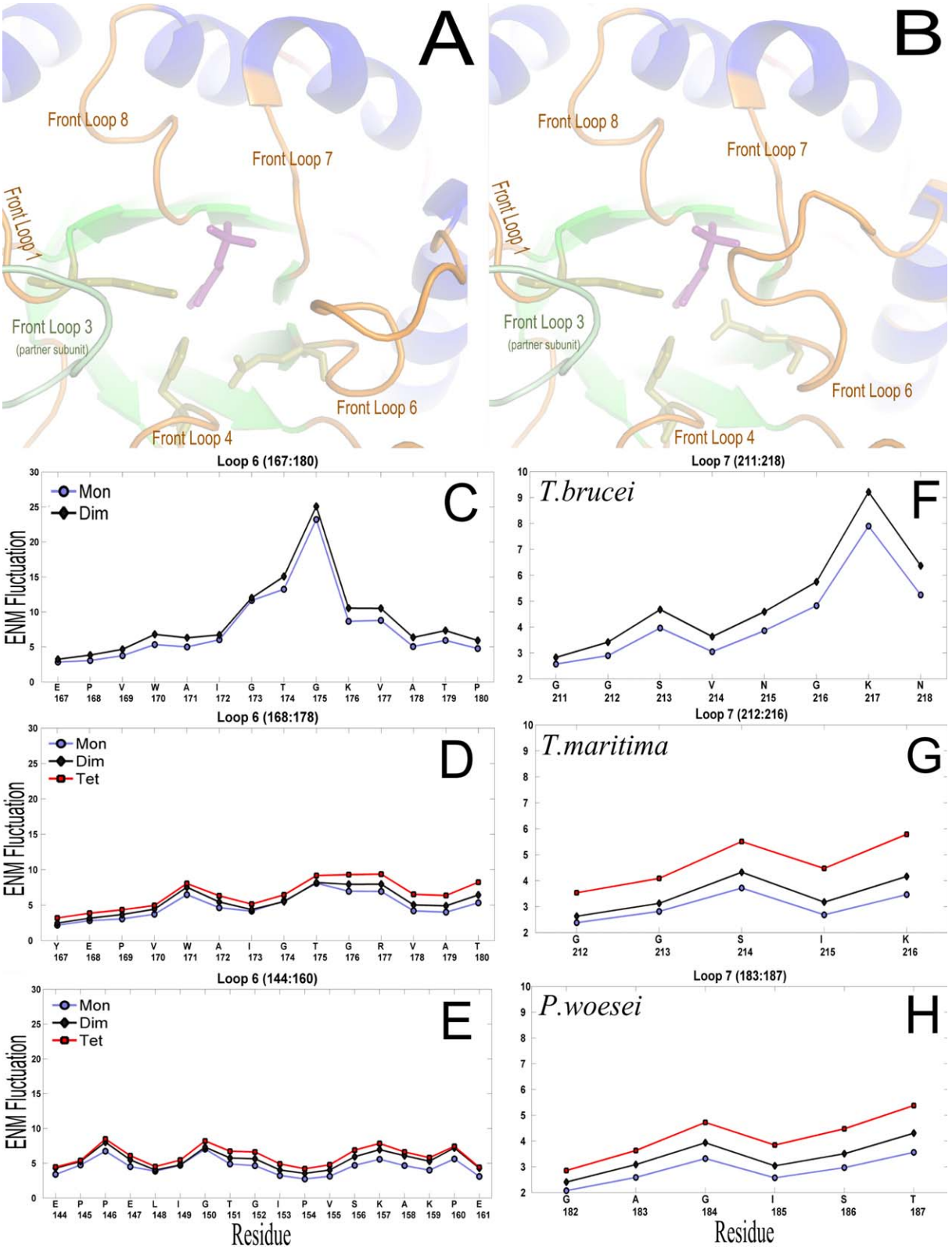

Figure 7. Differences of fluctuations of functional loops between the open and closed conformations. (A) Arrangement of functional loops 6, 7, and 8 around the catalytic pocket in the open conformation (based on *S. cerevisiae* open TIM structure PDB 1YPI) where the substrate (pink) is inserted at the catalytic site by superimposing the open and closed conformations. (B) The same arrangement in the closed conformation (based on *S. cerevisiae* TIM structure PDB 2YPI). (C, D, E) Fluctuations of functional Loop 6; (F, G, H) Fluctuations of functional Loop 7.

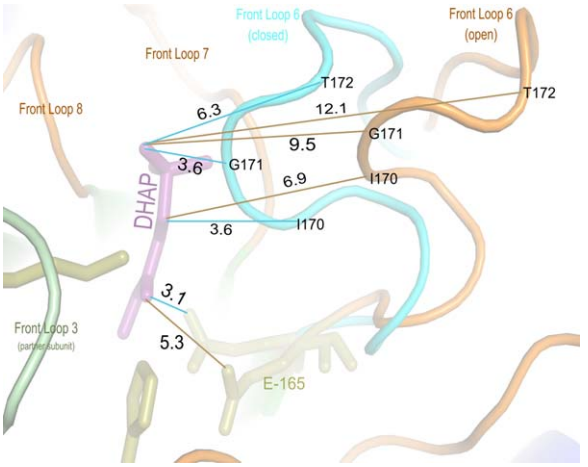

Figure 8. Changes in distances between substrate and different residues of the "phosphate gripper" between the open (orange) and closed (cyan) conformations. The residue indexing and open and closed conformations of the loops were generated using PyMol and the *S. cerevisiae* structure 1YPI (open conformation) and 7TIM (closed conformation). The excursions of the residues themselves in the "phosphate gripper" toward the catalytic pocket are: A169 3.0Å, I170 4.2Å, G171 6.7Å, T172 6.7Å, G173 8.0Å, L174 5.0Å, A175 4.3Å, and A176 1.6Å. Colors for lines: orange—the distance between the substrate and the residues for the open conformation of Loop 6, cyan—the distance between the substrate and the residues with the closed conformation of Loop 6.

fluctuation than Loop 6 in panels D and E. This implies that Loop 6 of *T. brucei* TIM has higher fluctuation than that of *T. maritima* and *P. woesei* TIM structures. Comparatively smaller fluctuations of this loop in panels D and E is a result of an overall increase in the stability in the hyperthermophilic TIM structures (PDBs 1B9B and 1HG3, respectively). The second aspect of these fluctuations in panels C, D, and E is that dimerization increases the mobility of this loop and tetramerization in hyperthermophilic organisms increases this mobility even further.

Panels F, G, and H of Figure 7 show that the average ENM fluctuations of Loop 7 in each case increase after dimerization, and even further after tetramerization. Moreover, in the open structure of mesophilic *T. brucei* TIM, Loop 7 has higher overall fluctuations than that of the closed structures of hyperthermophilic *T. maritima* and *P. woesei*. It has been found from experiments that Loop 7 synchronizes its motions with the two hinge regions of Loop 6 to drive the dynamics of Loop 6, whose motions are important for substrate trapping, catalysis, and product release.[10,11] Therefore, it implies that reduced fluctuations of this loop in the closed structures (panels G and H) is important to facilitate the catalytic mechanism and the required coordination with Loop 6 that to be discussed in a subsequent "Concerted motions of functional loops" section.

From the results above we conclude that tetramerization in hyperthermophilic organisms is required not only for structural stability but also for functional viability for survival in the thermally noisy extreme environment where those organisms adapted to be functional.

Reduced stability and functionality of an engineered monomeric TIM

Figure 9 compares the flexibility of different interface and functional loops in an engineered monomer monoTIM, and monomeric and dimeric conformations of *T. brucei* TIM. The engineered monomer has a shortened Loop 3, with eight residues from the C-terminus of *T. brucei* TIM having been removed to prevent its dimerization at this interface. Figure 9(E) shows how the shortening of Loop 3 has reduced the fluctuations of this loop in monoTIM. Other two interface loops 1 and 2 show increased mobility as a result. This has two consequences for the catalytic loop fluctuations. First, the patterns of fluctuations of loops 6 and 8 have changed in monoTIM. Second, the fluctuations of Loop 6 in monoTIM are significantly damped down, but the catalytically important Glu165 fluctuation has increased fluctuations. This reduced stability of Glu 165 may be a contributing factor in the diminished catalytic activity of monoTIM. Also, the damped down mobility of the "phosphate gripper" region [Figure 9(F), 171:178 – AIGTGKVA] in monoTIM may decrease its substrate hunting capability. This complies with the experimental results that showed Loop 6 flexibility to be essential for substrate recuritment.[10,11] Also, Figure 9(C) shows that the catalytic Lys loses its required rigidity in the engineered monomeric TIM monoTIM. This could also be a contributing factor to the reduced catalytic activity of monoTIM.

Engineered monoTIM has similar fluctuations as that of a monomer of a *T. brucei* TIM though it is reduced compared to the dimeric counterpart. It has been found from experiments that Loop 7 synchronizes its motions with the two hinge regions of Loop 6 to drive the dynamics of Loop 6, whose motion is important for substrate trapping, catalysis, and product release.[10,11] Therefore, the residual activity of monoTIM implies that the decreased fluctuations of Loop 7 are insufficient to generate the Loop 6 dynamics for the reduced substrate catalysis.[47]

Concerted motions of functional loops

Correlations between Loop 6 and Loop 7 dynamics. Different experiments have shown that Loop 7 plays a crucial role in the concerted motions of the N and C-terminal hinge residues of catalytic Loop 6, essential to maintain the high efficiency of

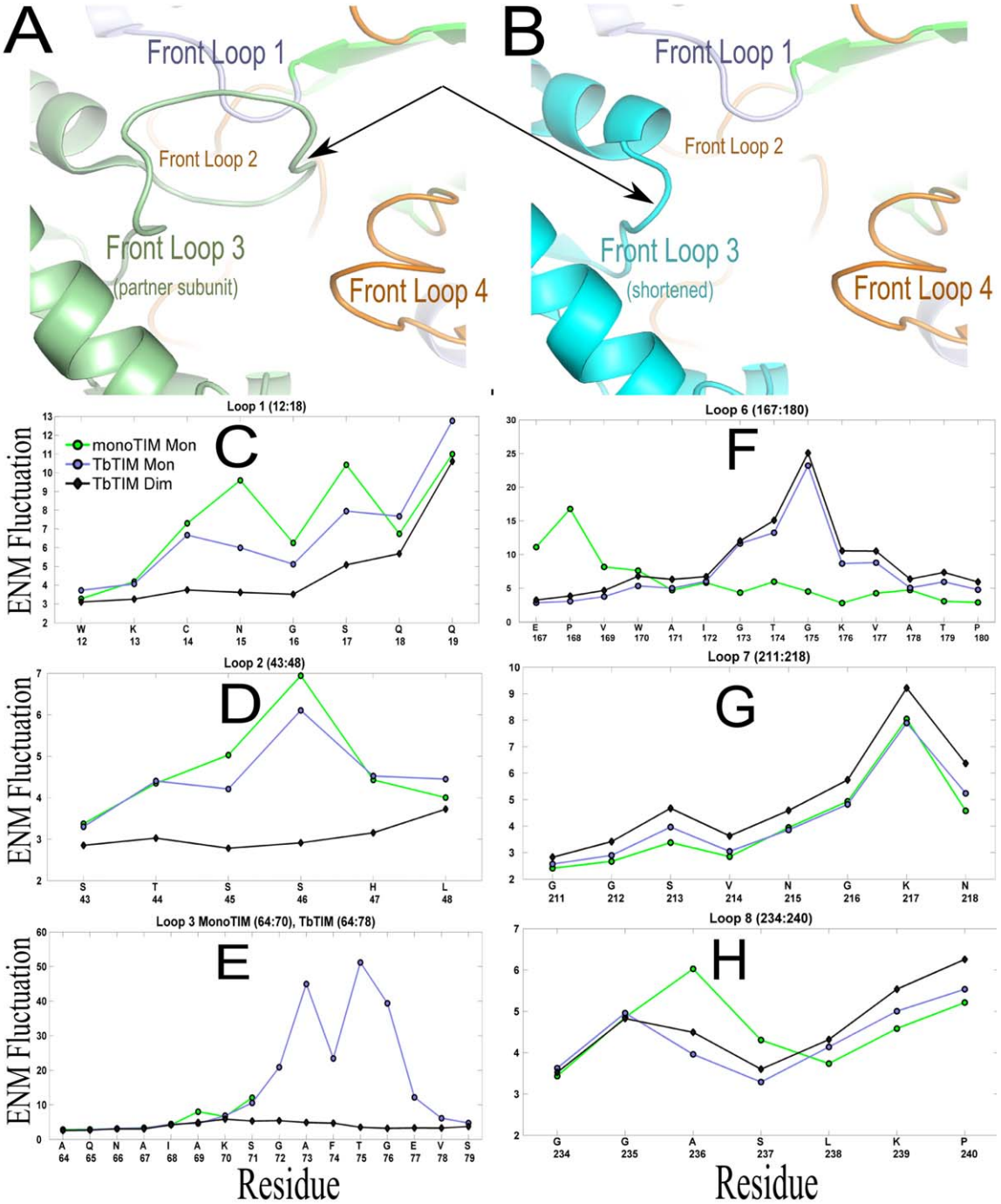

Figure 9. Changes in fluctuations of the interface and functional loops. (A) Ribbon diagram of the interdigitation of front loops 1 and 4 with the front Loop 3 from the partner subunit. (B) Ribbon diagram of front loops 1 and 4 with the shortened front Loop 3 from a hypothetical partner subunit. Loop 3 is shown by an arrow in A and B. (C, D, E, F, G, H) Fluctuations of loops 1, 2, 3, 6, 7, and 8 are shown, respectively.

TIM production.[48] Our analysis of TIM dynamics by ENM detects the parts of Loop 6 and Loop 7 where their motions are highly correlated and shows how they are maintained for different oligomerization states. Supporting Information Table SII shows the significant correlations between different parts of loops 6 and 7. It is evident that the "phosphate gripper" region of Loop 6 has the highest correlation with Loop 7 in each oligomeric state.

Correlations between Loop 6 and Loop 8 dynamics. We also computed the correlation between motions of Loop 6 and Loop 8. Supporting Information Table SIII details these values for the four structures. The "phosphate gripper" region of Loop 6 is highly correlated with Loop 8 in the mesophilic dimeric TIM structure TbTIM. However, this correlation is substantially reduced in the engineered monomeric TIM monoTIM. Between the two

Table I. *Significant Overlaps (> 0.40) of Modes of ENM Motions Between Chains in the Tetrameric* P. woesei *TIM*[a]

Mode #	1	2	3	4	5	Mode #	1	2	3	4	5
	Type 1 dimeric Chain A versus Chain B						Type 2 Dimeric Chain A versus Chain C				
1					0.41	1					
2						2		0.77			
3			0.94	0.62		3		0.41			
4			0.64	0.88		4					
5					0.68	5					0.71
	Tetrameric Chain A versus Chain B						Tetrameric Chain A versus Chain C				
1	0.52					1		0.42		0.42	
2						2		0.82			0.76
3			0.59	0.47		3					
4			0.45			4					
5						5		0.74			0.89
	Tetrameric Chain A versus Chain D						Tetrameric Chain B versus Chain C				
1			0.45			1			0.43		
2						2					
3	0.45		0.54			3	0.43		0.55		
4				0.96		4				0.95	
5						5					
	Tetrameric Chain B versus Chain D						Tetrameric Chain C versus Chain D				
1						1	0.52				
2	0.42	0.83		0.73		2					
3						3			0.59	0.46	
4	0.41					4			0.47		
5		0.77		0.89		5					

[a] Overlaps between chains A and B in Type 1 dimeric structure are larger than it is in Type 2 dimeric structure. Overlaps between the chains across the center (chains A compared with chain D and chains B with C) is higher than any two interface forming chains (chain A compared to B; chain A to C; chain B to D; and chains C to D).

hyperthermophilic structures, TmTIM and PwTIM, the first structure maintains this high correlation, but the second one does not.

Correlations between Loop 7 and Loop 8 dynamics. Supporting Information Table SIV shows the details of the correlations between these two loops for the four structures. Interestingly, the direction of correlation has changed in the engineered monomeric TIM monoTIM from that of the dimeric TIM TbTIM. On the other hand, both hyperthermophilic TIM structures TmTIM and PwTIM maintain high positive correlations between these two loops. This could imply that correlations between loops 6 and 7, and between loops 6 and 8, are stronger in TmTIM and PwTIM compared to monoTIM and TbTIM. The significance of this lies in the following proposition: higher oligomerization increases functional loop correlations in the tetrameric structure, making it more efficient than its dimeric counterpart.

Overlap of modes of ENM motions

Our computation shows that the overlap of motions between chain A and chain B in a hypothetical Type 1 dimeric structure is much higher than the overlap between chain A and chain C of a hypothetical Type 2 dimer for *P.woesei* TIM, shown in Table I. However, in the tetrameric structure, overlaps between the chains across the barrel are the highest, and they are almost symmetric for the two pairs—chain A compared with chain D and chain B compared with chain C.

Changes of loop motions with change in correlations of functional loop motions

The change in flexibilities of functional loops after oligomerization not only facilitates substrate binding but also increases the correlation between functional loop motions required for the synchrony of the catalytic mechanism. In tetrameric TIM, we can observe a higher rigidity in loops 1, 4, and 8, with higher flexibility in loops 6 and 7. The correlations between loops 6, 7, and 8 also increase overall in the tetrameric TIM structures.

In hyperthermophilic TIM, teramerization is required to achieve sufficient cohesion to carry out the catalysis. Two functionally inactive dimers come together to form a functionally active tetrameric

complex. This tetramerization increases functional loop fluctuations and their correlations as well.

Discussion

Motions of the interface loops and the functional loops are interdependent. Dimerization at the interface loops (front loops 1, 2, 3, and 4) changes not only their dynamics and correlations but also that of the functional loops (front loops 6, 7, and 8), making them highly efficient for substrate recruitment, catalytic activity, and product release. Tetramerization improves the functional loop dynamics and further enhances their coordination.

Interface loops 1, 2, 3, and 4: Dimerization of TIM brings the catalytic residue Lys on Loop 1 and His on Loop 4 closer to the catalytic pocket. Also, it reduces the fluctuations of the interface loops, thus stabilizing the structure and facilitating the required motions among the interface loops 6, 7, and 8.

Functional loops 6, 7 and 8: Motions of loops 6, 7, and 8 depend on two events:

- Oligomerization: Motions of these loops increase because of oligomerization which is necessary for substrate recruitment and product release.
- Substrate binding: Motions of these loops decrease after substrate binding which is necessary to protect the catalytic cavity from penetration of any unwanted small molecules.

Leu on Loop 8 responsible for the highly specific shape of the TIM catalytic cavity is believed to be stabilized because of the reduced Loop 8 motions after substrate binding.

Correlation of the functional loops. Loops 6 and 7 maintain a high correlation, regardless of the oligomeric state of TIM. Interestingly, in different oligomeric states, Loop 7 changes its highest correlation value with different parts of Loop 6. This might imply that although different oligomeric states have high correlation between Loop 7 and different parts of Loop 6, Loop 7 of the functionally active oligomers (monoTIM, TbTIM dimer, TmTIM tetramer, PwTIM tetramer) achieves the expected overall high correlation in the required region of Loop 6.

Catalytic competency of TIM hinges on two important things: (i) stability of Loop 1 and Loop 4 (catalytic residues Lys and His on Loop 1 and Loop 4, respectively); and (ii) flexibility and coordination of Loop 6 and Loop 7. Tetramerization increases both as dimerization does. Hence, the hyperthermophilic organisms adapted to survive in the extremely high temperature through the tetramerization of this structure.

Thus dimerization can be considered as a switch for TIM structures that helps these structures to achieve functionally important motions. In addition, tetramerization improves the stability of the structure and also enhances the required structural coordination. Closed structures have reduced Loop 6 fluctuations compared to the open structures. This means that higher fluctuation in the open structure enables the structure to reach about farther in its vicinity to recruit substrate. In the closed structure, the residual fluctuations of Loop 6 retain the proper dynamics to assist the catalysis in a safe catalytic pocket.[8,49]

To summarize, the computations and analyses that we have carried out here reveal underlying reasons of some of the previous experimental findings about the dynamics of the functional loops of the TIM structures in different oligomeric states. The computations further show details of the allosteric regulation of the dynamics of the functional loops. Our results also indicate that tetramerization increases the stability of the interface loops, the flexibility of the functional loops, especially loops 6 and 7, and the coordination between them (loops 6 and 7), all of which may be important for the hyperthermophilic organisms to survive at extreme temperatures.

Materials and Methods

Data set preparation

TIM structure database. We have downloaded 121 TIM structures from the Protein Data Bank (PDB) (www.pdb.org)[50] dated 10/14/2011. After extracting each chain from the structures we have a database of 307 individual TIM chains. This database contains monomeric chains (engineered or mutated so that dimerization does not happen), dimeric chains (either wild type or mutated), and tetrameric chains for four hyperthermophilic organisms—1B9B (*T. maritima*), 1HG3 (*P. woesei*), 1W0M (*T. tenax*), and 2H6R (*M. jannaschii*). Functional Loop 6 is the most disordered region of the TIM enzyme, and many structures are missing this loop, either in part or in its entirety. After removing all chains with missing Loop 6, we have 267 chains remaining. These PDB Ids are listed in the Supporting Information.

We have normalized these chains by aligning each chain with chain A of the yeast PDB structure 2YPI. PCA shown in Figure 1 is based on this set of selected TIM chains.

PDB structures to measure the allosteric effect of oligomerization: We have selected four PDB structures to observe the allosteric effect of TIM oligomerization: 1MSS (Engineered monomer from *T. brucei* TIM), 1TPE (*T. brucei* TIM), 1B9B (*T. maritima*), and 1HG3 (*P. woesei*). The detailed descriptions of

these structures can be found in the Supporting Information.

Principal component analysis (PCA)—exploring the TIM structure space by PCA

PCA—Principal Component Analysis. It is a multivariate technique to analyze data where the observations are described quantitatively by a set of inter-correlated variables. The goals are to (i) extract the most important information from the data; (ii) remove noise and compress the size of the data set by keeping only the most important information; (iii) simplify the description of the dataset; and (iv) analyze the structure of the observations and the variables. This method generates a set of new orthogonal variables called principal components (PCs). Each PC is a linear combination of the original variables. Hence, PCA can be considered as a mapping of the data points from the original variable space to the PC space. PCs are computed in such a way that when each data point is projected onto PC1, the resulting values form a new variable that has the maximum variance among all possible choices for the first axis. Similarly, when each data point is projected on PC2, the resulting values form another new variable that has the maximum variance among all possible choices for the second axis, and so forth. While there are a large number of PCs, usually only a few PCs are sufficient to understand the structure of the data.[51] The mathematical derivation of the PCs is summarized in the Supporting Information.

Exploring the TIM structure space by PCA. The coordinates of 14 residues that span the Loop 6 residues are extracted from each of the 267 chains of the TIM structure dataset, normalized TIMchains. The motifs that are used to find the start of Loop 6 are: EPIWAIG, EPVWSIG, EPPELIG, EPLWAIG, EPLWAIG, EPVWAAT, EPVWAIT, EPVWAVG, EPLFAIG, EAVWAIG, and DPVWAIG.

Here, the 14 residue positions on Loop 6 are the variables of the data set for PCA. The 267 segments, each spanning the Loop 6 of each structure, are the data points. We use *princomp* function of Matlab Statistical Toolbox to compute the PCs (PC1, PC2, PC3 ...) (2010a, The MathWorks, Natick, MA).

Modeling dynamics

Given two structures, we compute their normal modes using the Anisotropic Network Model (ANM);[52] we have chosen a cutoff value of 12Å. The normal modes for each structure are represented as a set of vectors. The normal modes from one ANM model can be compared to the normal modes from another ANM model using the following equation which describes the "Overlap" between the directions of the *i*th mode of one model and the *j*th mode of another model as described by Tama and Sanejouand[53] and Leo-Macias et al.[54]

$$O_{ij}=\frac{|\mathbf{M_i}.\mathbf{M_j}|}{\|\mathbf{M_i}\|\|\mathbf{M_j}\|}$$

We adapted these metrics to compare the functional loop dynamics of TIM structures of different oligomeric states. We select the equal length matching segments of loops from a specific protein pair and extract the normal modes for only those segments from the ENM results. Then we compute Overlap for each of the re-orthonormalized sets of modes.

Acknowledgment

A.R.K. and R.L.J. contributed to the design, execution, and writing of this work.

References

1. Maes D, Zeelen JP, Thanki N, Beaucamp N, Alvarez M, Thi MH, Backmann J, Martial JA, Wyns L, Jaenicke R, Wierenga RK (1999) The crystal structure of triosephosphate isomerase (TIM) from Thermotoga maritima: a comparative thermostability structural analysis of ten different TIM structures. Proteins 37: 441–453.
2. Walden H, Bell GS, Russell RJ, Siebers B, Hensel R, Taylor GL (2001) Tiny TIM: a small, tetrameric, hyperthermostable triosephosphate isomerase. J Mol Biol 306:745–757.
3. Walden H, Taylor GL, Lorentzen E, Pohl E, Lilie H, Schramm A, Knura T, Stubbe K, Tjaden B, Hensel R (2004) Structure and function of a regulated archaeal triosephosphate isomerase adapted to high temperature. J Mol Biol 342:861–875.
4. Gayathri P, Banerjee M, Vijayalakshmi A, Azeez S, Balaram H, Balaram P, Murthy MR (2007) Structure of triosephosphate isomerase (TIM) from *Methanocaldococcus jannaschii*. Acta Crystallogr D Biol Crystallogr 63:206–220.
5. Kurkcuoglu Z, Bakan A, Kocaman D, Bahar I, Doruker P (2012) Coupling between catalytic loop motions and enzyme global dynamics. PLoS Comput Biol 8: e1002705.
6. Cansu S, Doruker P (2008) Dimerization affects collective dynamics of triosephosphate isomerase. Biochemistry 47:1358–1368.
7. Alakent B, Baskan S, Doruker P (2011) Effect of ligand binding on the intraminimum dynamics of proteins. J Comput Chem 32:483–496.
8. Kurkcuoglu O, Jernigan RL, Doruker P (2006) Loop motions of triosephosphate isomerase observed with elastic networks. Biochemistry 45:1173–1182.
9. Knowles JR (1991) Enzyme catalysis: not different, just better. Nature 350:121–124.
10. Rozovsky S, Jogl G, Tong L, McDermott AE (2001) Solution-state NMR investigations of triosephosphate isomerase active site loop motion: ligand release in relation to active site loop dynamics. J Mol Biol 310: 271–280.
11. Rozovsky S, McDermott AE (2001) The time scale of the catalytic loop motion in triosephosphate isomerase. J Mol Biol 310:259–270.

12. Casteleijn MG, Alahuhta M, Groebel K, El-Sayed I, Augustyns K, Lambeir AM, Neubauer P, Wierenga RK (2006) Functional role of the conserved active site proline of triosephosphate isomerase. Biochemistry 45: 15483–15494.
13. Alahuhta M, Casteleijn MG, Neubauer P, Wierenga RK (2008) Structural studies show that the A178L mutation in the C-terminal hinge of the catalytic loop-6 of triosephosphate isomerase (TIM) induces a closed-like conformation in dimeric and monomeric TIM. Acta Crystallogr D Biol Crystallogr 64:178–188.
14. Eaazhisai K, Balaram H, Balaram P, Murthy MR (2004) Structures of unliganded and inhibitor complexes of W168F, a Loop6 hinge mutant of Plasmodium falciparum triosephosphate isomerase: observation of an intermediate position of loop6. J Mol Biol 343:671–684.
15. (2012) The PyMOL molecular graphics system, version 1.4, Schrödinger, LLC.
16. Wierenga RK, Kapetaniou EG, Venkatesan R (2010) Triosephosphate isomerase: a highly evolved biocatalyst. Cell Mol Life Sci 67:3961–3982.
17. Joseph D, Petsko GA, Karplus M (1990) Anatomy of a conformational change: hinged "lid" motion of the triosephosphate isomerase loop. Science 249:1425–1428.
18. Noble ME, Zeelen JP, Wierenga RK (1993) Structures of the "open" and "closed" state of trypanosomal triosephosphate isomerase, as observed in a new crystal form: implications for the reaction mechanism. Proteins 16:311–326.
19. Parthasarathy S, Ravindra G, Balaram H, Balaram P, Murthy MR (2002) Structure of the Plasmodium falciparum triosephosphate isomerase-phosphoglycolate complex in two crystal forms: characterization of catalytic loop open and closed conformations in the ligand-bound state. Biochemistry 41:1317813–131788.
20. Norledge BV, Lambeir AM, Abagyan RA, Rottmann A, Fernandez AM, Filimonov VV, Peter MG, Wierenga RK (2001) Modeling, mutagenesis, and structural studies on the fully conserved phosphate-binding loop (loop 8) of triosephosphate isomerase: toward a new substrate specificity. Proteins 42:383–389.
21. Rozovsky S, Jogl G, Tong L, McDermott AE (2001) Solution-state NMR investigations of triosephosphate isomerase active site loop motion: ligand release in relation to active site loop dynamics. J Mol Biol 310: 271–280.
22. Seeburg PH, Colby WW, Capon DJ, Goeddel DV, Levinson AD (1984) Biological properties of human c-Ha-ras1 genes mutated at codon 12. Nature 312:71–75.
23. Reinstein J, Vetter IR, Schlichting I, Rosch P, Wittinghofer A, Goody RS (1990) Fluorescence and NMR investigations on the ligand binding properties of adenylate kinases. Biochemistry 29:7440–7450.
24. Moller W, Amons R (1985) Phosphate-binding sequences in nucleotide-binding proteins. FEBS Lett 186:1–7.
25. Wierenga RK, Terpstra P, Hol WG (1986) Prediction of the occurrence of the ADP-binding beta alpha beta-fold in proteins, using an amino acid sequence fingerprint. J Mol Biol 187:101–107.
26. Lowry DF, Ahmadian MR, Redfield AG, Sprinzl M (1992) NMR study of the phosphate-binding loops of Thermus thermophilus elongation factor Tu. Biochemistry 31:2977–2982.
27. Saraste M, Sibbald PR, Wittinghofer A (1990) The P-loop—a common motif in ATP- and GTP-binding proteins. Trends Biochem Sci 15:430–434.
28. Norledge BV, Lambeir AM, Abagyan RA, Rottmann A, Fernandez AM, Filimonov VV, Peter MG, Wierenga RK (2001) Modeling, mutagenesis, and structural studies on the fully conserved phosphate-binding loop (loop 8) of triosephosphate isomerase: toward a new substrate specificity. Proteins 42:383–389.
29. Jogl G, Rozovsky S, McDermott AE, Tong L (2003) Optimal alignment for enzymatic proton transfer: structure of the Michaelis complex of triosephosphate isomerase at 1.2-A resolution. Proc Natl Acad Sci USA 100:50–55.
30. Kursula I, Salin M, Sun J, Norledge BV, Haapalainen AM, Sampson NS, Wierenga RK (2004) Understanding protein lids: structural analysis of active hinge mutants in triosephosphate isomerase. Protein Eng Des Sel 17:375–382.
31. Venkatesan R, Alahuhta M, Pihko PM, Wierenga RK (2011) High resolution crystal structures of triosephosphate isomerase complexed with its suicide inhibitors: the conformational flexibility of the catalytic glutamate in its closed, liganded active site. Protein Sci 20:1387–1397.
32. Gerstein M, Lesk AM, Chothia C (1994) Structural mechanisms for domain movements in proteins. Biochemistry 33:6739–6749.
33. Gerstein M, Anderson BF, Norris GE, Baker EN, Lesk AM, Chothia C (1993) Domain closure in lactoferrin. Two hinges produce a see-saw motion between alternative close-packed interfaces. J Mol Biol 234:357–372.
34. Bahar I, Atilgan AR, Erman B (1997) Direct evaluation of thermal fluctuations in proteins using a single-parameter harmonic potential. Fold Des 2:173–181.
35. Bahar I, Erman B, Haliloglu T, Jernigan RL (1997) Efficient characterization of collective motions and interresidue correlations in proteins by low-resolution simulations. Biochemistry 36:13512–13523.
36. Doruker P, Jernigan RL, Bahar I (2002) Dynamics of large proteins through hierarchical levels of coarse-grained structures. J Comput Chem 23:119–127.
37. Jernigan RL, Demirel MC, Bahar I (1999) Relating Structure to Function through the Dominant Modes of Motion of DNA Topoisomerase II Int J Quant Chem (B Pullman Memorial Volume) 175:301–312.
38. Jernigan RL, Yang L, Song G, Doruker P (2008) Elastic Network Models of Coarse-Grained Proteins Are Effective for Studying the Structural Control Exerted over Their Dynamics. In: Coarse-graining of condensed phase and biomolecular systems G Voth (Ed) Taylor and Francis Group LLC 237–254.
39. Keskin O, Durell SR, Bahar I, Jernigan RL, Covell DG (2002) Relating molecular flexibility to function: a case study of tubulin. Biophys J 83:663–680.
40. Kim MK, Chirikjian GS, Jernigan RL (2002) Elastic models of conformational transitions in macromolecules. J Mol Graph Model 21:151–160.
41. Kim MK, Jernigan RL, Chirikjian GS (2003) An elastic network model of HK97 capsid maturation. J Struct Biol 143:107–117.
42. Kurkcuoglu O, Jernigan RL, Pemra D (2005) Collective dynamics of large proteins from mixed coarse-grained elastic network model. QSAR Combinatorial Science 24:443–448.
43. Kurkcuoglu O, Kurkcuoglu Z, Doruker P, Jernigan RL (2009) Collective dynamics of the ribosomal tunnel revealed by elastic network modeling. Proteins 75:837–845.
44. Wang Y, Rader AJ, Bahar I, Jernigan RL (2004) Global ribosome motions revealed with elastic network model. J Struct Biol 147:302–314.
45. Yang L, Song G, Jernigan RL (2007) How well can we understand large-scale protein motions using normal

modes of elastic network models? Biophys J 93:920–929.
46. Yang L, Song G, Jernigan RL (2009) Protein elastic network models and the ranges of cooperativity. Proc Natl Acad Sci USA 106:12347–12352.
47. Borchert TV, Kishan KV, Zeelen JP, Schliebs W, Thanki N, Abagyan R, Jaenicke R, Wierenga RK (1995) Three new crystal structures of point mutation variants of monoTIM: conformational flexibility of loop-1, loop-4 and loop-8. Structure 3: 669–679.
48. Wang Y, Berlow RB, Loria JP (2009) Role of loop-loop interactions in coordinating motions and enzymatic function in triosephosphate isomerase. Biochemistry 48:4548–4556.
49. Kurkcuoglu O, Turgut OT, Cansu S, Jernigan RL, Doruker P (2009) Focused functional dynamics of supramolecules by use of a mixed-resolution elastic network model. Biophys J 97:1178–1187.
50. Berman HM, Westbrook J, Feng Z, Gilliland G, Bhat TN, Weissig H, Shindyalov IN, Bourne PE (2000) The protein data bank. Nucleic Acids Res 28:235–242.
51. Abdi H, Williams LJ (2010) Principal Component Analysis. WIREs Comput Stat 2:433–459.
52. Atilgan AR, Durell SR, Jernigan RL, Demirel MC, Keskin O, Bahar I (2001) Anisotropy of fluctuation dynamics of proteins with an elastic network model. Biophys J 80:505–515.
53. Tama F, Sanejouand YH (2001) Conformational change of proteins arising from normal mode calculations. Prot Eng 14:1–6.
54. Leo-Macias A, Lopez-Romero P, Lupyan D, Zerbino D, Ortiz AR (2005) An analysis of core deformations in protein superfamilies. Biophys J 88:1291–1299.